Covalent Binding of Three Epoxyalkyl Xylosides to the Active Site of *endo*-1,4-Xylanase II from *Trichoderma reesei*[†,‡]

Riikka Havukainen,[§,∥] Anneli Törrönen,[§,⊥] Tuomo Laitinen, and Juha Rouvinen*

Department of Chemistry, University of Joensuu, P.O. Box 111, FIN-80101 Joensuu, Finland

Received December 28, 1995; Revised Manuscript Received April 29, 1996[⊗]

ABSTRACT: The three-dimensional structures of *endo*-1,4-xylanase II (XYNII) from *Trichoderma reesei* complexed with 4,5-epoxypentyl β-D-xyloside (X-O-C_5), 3,4-epoxybutyl β-D-xyloside (X-O-C_4), and 2,3-epoxypropyl β-D-xyloside (X-O-C_3) were determined by X-ray crystallography. High-resolution measurement revealed clear electron densities for each ligand. Both X-O-C_5 and X-O-C_3 were found to form a covalent bond with the putative nucleophile Glu86. Unexpectedly, X-O-C_4 was found to bind to the putative acid/base catalyst Glu177. In all three complexes, clear conformational changes were found in XYNII compared to the native structure. These changes were largest in the X-O-C_3 complex structure.

Due to its potential applications, for example, in the pulp bleaching and food and feed industry, the enzymatic hydrolysis of xylan has recently drawn more and more attention. *endo*-1,4-Xylanase II from *Trichoderma reesei* (XYNII)[1] is one of the best characterized hemicellulolytic enzymes (Tenkanen et al., 1992). XYNII cleaves the β-1,4-glycosidic linkage between two xylose residues (Figure 1a). The enzyme is an endohydrolase consisting of a single 190 residue polypeptide chain folded into one domain composed of two β-sheets packed parallel to each other and one α-helix. The two separate β-sheets are oriented at almost 90° angles relative to one another, forming an overall shape that has been described as similar to a right hand. The two β-sheets form the fingers, and the twisted part of the β-sheets and the α-helix form the palm. The concave face of the twisted β-sheets forms the substrate binding site. The long loop between two β-strands makes a "thumb" which partly closes the cleft (Figure 2a).

Two glutamic acid residues located on the different sites of the substrate binding cleft of XYNII are putative catalytic residues (Törrönen et al., 1994). Both of the residues are completely conserved among XYNII homologous xylanases (family 11/G) (Törrönen et al., 1993a). Glu177 is probably the so-called acid/base catalyst whereas Glu86 is likely to be the nucleophile. In a previous paper (Törrönen et al., 1995) we reported that a change in pH caused a striking conformational change in the active site of XYNII, especially in the position of the catalytic residue Glu177. The change in Glu177 brings it closer to the substrate. XYNII probably

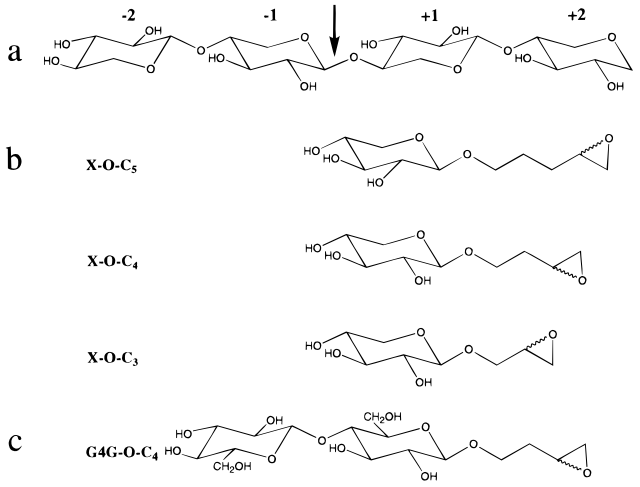

FIGURE 1: (a) Chemical structure of a model substrate, xylotetraose. The point of cleavage by XYNII at a 1,4-β-D-glucosidic bond is marked by an arrow. The numbers −2, −1, +1, and +2 refer the different subsites of the enzyme. (b) Chemical structures of XYNII ligands X-O-C_5, X-O-C_4, and X-O-C_3. (c) Chemical structures of *Bacillus* 1,3-1,4-β-glucanase ligand G4G-O-C_4 (Keitel et al., 1993).

has five subsites, −2, −1, +1, +2, and +3, where positive numbers represent reducing end direction and negative nonreducing end direction. The cleavage takes place between subsites −1 and +1 (Figure 1a). The side chain Trp18 forms subsite −2, in which the residues Tyr77 and Tyr171 can be hydrogen-bonded to the substrate. Subsites −1 and +1 were expected to have no potential interactions other than those of the catalytic residues Glu86 and Glu177. The residues Tyr179 and Tyr96 are thought to determine subsites +2 and +3.

During the last few years many three-dimensional structures of glycosyl hydrolases have been determined (Davies et al., 1995) but fewer complex structures have been published. This is probably due to the difficulties in synthesizing complex oligosaccharide molecules, and the ligands used have often had an affinity too low toward the studied enzymes (Törrönen et al., 1995). One new potential alternative is to use irreversible, mechanism-based inhibitors, for example, epoxyalkyl glycosides. The covalently-binding epoxyalkyl glycosides have proved to be beneficial when

† Supported by the Academy of Finland and the Finnish Graduate School "Protein Structure and Function" (R.H.).

‡ Crystallographic coordinates have been deposited in the Brookhaven Protein Data Bank (reference 1RED, 1REE, 1REF).

* To whom correspondence should be addressed; Fax 358-73-151 3390.

§ The equal first authors.

∥ Present address: Universität Graz, Institut für Physikalische Chemie, Heinrichstrasse 28, A-8010 Graz, Austria.

⊥ Present address: EMBL, Meyerhofstrasse 1, D-69012 Heidelberg, Germany.

⊗ Abstract published in *Advance ACS Abstracts,* July 1, 1996.

[1] Abbreviations: XYNII, *endo*-1,4-β-xylanase II from *Trichoderma reesei*; X-O-C_5, 4,5-epoxypentyl β-D-xyloside; X-O-C_4, 3,4-epoxybutyl β-D-xyloside; X-O-C_3, 2,3-epoxypropyl β-D-xyloside; G4G-O-C_4, 3,4-epoxybutyl β-D-cellobioside.

S0006-2960(95)03052-2 CCC: $12.00

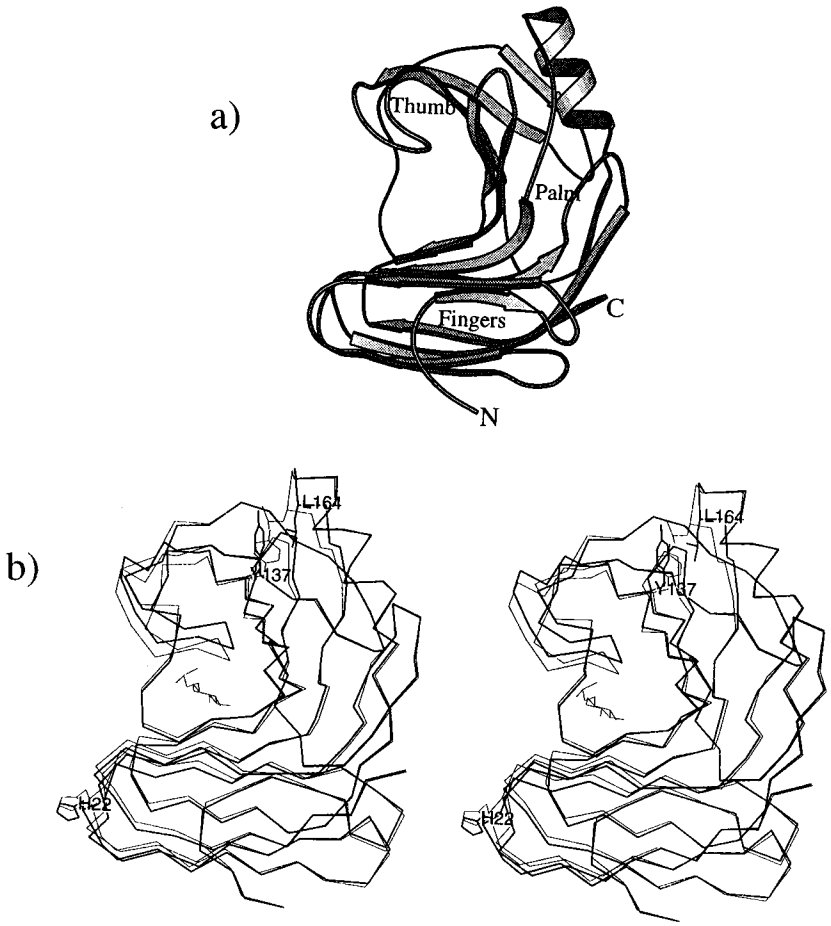

FIGURE 2: (a) Schematic drawing of XYNII (drawn using Molscript; Kraulis, 1991). (b) Superimposed C_α skeletons of two XYNII molecules in stereo, native A (pH 4.5) (thick lines) and X-O-C_3 complex B molecule (thin line) showing the conformational change caused by ligand binding. The ligand in the active site is from the complex structure X-O-C_3.

studying the ligand binding and reaction mechanisms of glycosyl hydrolases. It has been suggested that the epoxyl oxygen acts as the target for the nucleophilic attack from the acidic catalytic residue and the sugar moieties attached to the aglycon can bind to the subsites of the enzyme in the same manner as the natural substrate (Høj et al., 1989).

While a number of kinetics studies using epoxy-based inhibitors have been reported (Høj et al., 1989, 1991, 1992; Clarke et al., 1988), there have been few complex crystal structure analyses using these covalently-binding alkylating agents. The complex structures of *Bacillus* H(A16-M) hybrid 1,3-1,4-glucanase with the covalently-bound inhibitor 3,4-epoxybutyl β-D-cellobioside (G4G-O-C_4) (Figure 1c) have been determined at 2.0 Å resolution. In this study the ligand formed the covalent bond with the catalytic nucleophilic residue, Glu105. A long butyl linker is strongly twisted and makes no close contacts to active-site atoms. The position of the hydroxyl group of the β-hydroxy ester was not visible in the electron density map (Keitel et al., 1993).

Barley 1,3-β-D-glucanase isoenzyme GII complexed with the inhibitor 2,3-epoxypropyl β-laminaribioside has been determined at 2.8 Å resolution. The coordinates of this complex are not available in the Brookhaven data bank, and the electron density of the complex structure has not been presented. However, the ligand was found to form a covalent bond with the nucleophile Glu231 (Chen et al., 1995).

In this study the aim was to characterize the substrate binding cleft of xylanases by using the covalently-binding inhibitors. Interestingly, the observed ligand binding revealed also conformational changes in the protein, different binding modes, as well as new information about enzyme mechanism. We present here the results of the analysis of three complex structures of XYNII using the covalently-binding inhibitors 4,5-epoxypentyl β-D-xyloside (X-O-C_5), 3,4-epoxybutyl β-D-xyloside (X-O-C_4), and 2,3-epoxypropyl β-D-xyloside (X-O-C_3) (Figure 1b).

EXPERIMENTAL PROCEDURES

Inhibitors. The chemicals D-(+)-xylose, 4-penten-1-ol, 3-buten-1-ol, and 2-propen-1-ol were produced by Aldrich. The inhibitors used in this study were mixtures of diastereoisomers of epoxyalkyl β-D-xylosides. The epoxyalkyl β-D-xylopyranoses were prepared by a modified Koenigs-Knorr condensation of 2,3,4-tri-*O*-benzoyl-α-D-xylopyranosyl bromide with the appropriate unsaturated alcohol (4-penten-1-ol, 3-buten-1-ol, and 2-propen-1-ol). The epoxyalkyl β-D-xylopyranoses were purified by column chromatography performed on short columns (10−15 cm) of silica gel (Merck 70-230 mesh ASTM). Thin-layer chromatography (t.l.c.) was performed on silica gel 60 F254, precoated aluminium sheets (Merck Article 5554). The double bonds were oxidized to epoxides with *m*-chloroperoxybenzoic acid. The inhibitors were stored as their benzoylates in the dark at 4 °C. Prior to use, they were suspended in anhydrous MeOH to a concentration of 100 mg/mL and deacetylated with an equal volume of 1 M NaOMe at room temperature for 60 min with continuous mixing. The sample was then neutralized with 1 M HCl and filtered. The filtrate was evaporated

Table 1: Crystal and Diffraction Data

	X-O-C_5	X-O-C_4	X-O-C_3	benzoic acid
pH	6.1	5.3	5.8	5.8
no. of crystals	1	1	1	1
space group	$P2_1$	$P2_1$	$P2_1$	$P2_1$
a (Å)	81.94	81.84	82.34	81.66
b (Å)	60.96	60.81	60.88	60.81
c (Å)	38.04	38.09	37.89	38.12
β (deg)	94.03	94.20	94.28	94.41
max resolution (Å)	1.6	1.7	1.8	1.6
reflns collected	88 868	84 926	82 450	110 823
unique reflns	38 005	35 521	30 167	33 695
$I/\sigma(I)$	11.8	10.7	10.4	7.4
completeness (%)	76.0	85.1	85.5	67.3
resolution bin	1.6−1.7	1.7−1.8	1.8−1.9	1.6−1.7
$I/\sigma(I)$	1.9	2.4	2.7	1.6
completeness (%)	25.9	57.5	60.3	17.7
R_{merge} (%)[a]	7.28	9.07	8.60	9.41

[a] $R_{merge} = 100 \times \sum\sum|F^2(i) - \langle F^2(i)\rangle|/\sum\sum F^2(i)$.

to dryness under reduced pressure at 45 °C. The products were analyzed by using ^{1}H and ^{13}C NMR spectroscopy. The spectra of studied compounds showed the peaks corresponding the epoxyl compounds. In addition, the samples contained some impurities, mainly benzoic acid. Because of small yield, the products were not purified further but were used immediately for soaking.

Enzyme, Crystallization, and Soaking Experiments. Purification and crystallization of the native *endo*-1,4-xylanase II from *Trichoderma reesei* has earlier been described by Törrönen et al. (1992, 1993b). For soaking, 100 μL of saturated inhibitor solution in water was mixed with 100 μL of 5 M ammonium sulfate. The concentration of inhibitor in soaking solutions was estimated to be 50 mg/mL. The pH of the X-O-C_5, X-O-C_4, and X-O-C_3 soaking solutions were 6.1, 5.3, and 5.8, respectively. Before measuring, the native crystals were soaked in these solutions overnight.

Crystallography. The X-ray diffraction data were collected at 20 °C using an R-AXIS IIC imaging plate area detector mounted on a Rigaku RU200HB rotating anode generator using Cu Kα radiation. The current was set at 180 mA and the voltage at 50 kV. The oscillation method was used to measure diffraction intensities. Exposures of 10 min per 1° oscillation were used over the range of 180°. The observed decay during data collection was under 20%. The R-AXIS image plate data were scaled and processed with the R-AXIS software (Sato et al., 1992). The data collection statistics are given in Table 1. The complex molecules were refined with X-PLOR (Brünger et al., 1987). The native protein coordinates were used in the refinement of the complex structures since both the native and complexed protein had the same cell dimensions and belonged to the same space group, $P2_1$. For the complex structures with ligands X-O-C_5, X-O-C_4, and X-O-C_3 diffraction data in the range of 8.0−1.6 Å, 1.7 and 1.8 Å were used, respectively. The refinement cycles included energy minimization and individual *B* factor refinement. Fourier maps and model phases were calculated after each refinement cycle. $2|F_o| - |F_c|$ and $|F_o| - |F_c|$ were used as Fourier map coefficients. Some manual corrections in the side chain geometry and water position adjustment along with adding water molecules were made with program O (Jones et al., 1991) between the refinement cycles. The cutoff temperature factor for the water molecules was 60 Å^2. The final refinement statistics are given in Table 2.

Table 2: Summary of Refinement

	X-O-C_5	X-O-C_4	X-O-C_3	benzoic acid
resolution of data (Å)	8.0−1.6	8.0−1.6	8.0−1.8	8.0−1.6
R factor[a] (%)	18.0	18.1	18.1	19.9
reflns used	33 775	31 504	26 750	29 913
free *R* factor (%)	22.2	22.3	22.9	24.7
no. of non-H-atoms	3275	3222	3233	3258
protein	2960	2960	2960	2960
water	290	238	250	289
ligand	16	15	14	
benzoic acid	9	9	9	9
deviation from ideality				
bond lengths (Å)	0.006	0.006	0.005	0.005
bond angles (deg)	1.4	1.4	1.3	1.3
dihedrals (deg)	27.2	27.0	27.1	27.2
improper dihedrals (deg)	1.0	1.0	0.9	0.9
av *B* factors (Å^2)	20.8	21.5	22.4	18.7
main chain atoms	18.1	18.5	19.6	15.9
all protein atoms	19.3	19.9	21.0	17.1
water	35.0	35.8	38.4	34.4
ligand	30.2	36.5	23.9	
benzoic acid	42.9	54.7	48.9	43.9
PDB code	1RED	1REE	1REF	

[a] *R* factor $= \sum|F_o - F_c|/\sum F_o$.

RESULTS

Binding of the Inhibitors to the Active Site. The XYNII crystals belonged to the space group $P2_1$ and contained two enzyme molecules named as A and B in an asymmetric unit. The inhibitors were bound only to molecule B. No electron density was observed for any ligand in the active site of molecule A in all three complex structures. The omit difference electron density maps of the bound ligand and the corresponding glutamic acid residue are shown in Figure 3 together with the final atomic models after the structure refinement. The final maps showed very good electron densities for the ligands. For example, the electron density of the hydroxyl group formed of the ligands is visible in all of the three complex structures determined. The inhibitor solutions were a mixture of *R* and *S* stereoisomers. Based on the refined complex structures, the bound epoxy ligands X-O-C_5 and X-O-C_3 seem to be of the isomer *R* but X-O-C_4 could be either *R* or *S* isomer.

X-O-C_5 bound covalently to the catalytic residue Glu86. The covalent attachment is indicated by the continuous electron density in the side chain of Glu86 (Figure 3a). The xylose moiety is in the chair conformation and occupies subsite −2 and the twisted aglycon stretched over subsite −1. The torsion angles of the chain are all staggered or near staggered. The xylose unit forms hydrogen bonds between its hydroxyl groups and the side chains of the residues Tyr77 and Tyr171. The hydroxyl group of the hydroxyl ester formed is hydrogen-bonded to the residues Tyr88, Tyr77, and the catalytic residue Glu177. The ether oxygen also forms a hydrogen bond to the Tyr77. Trp18 contributes to the ligand binding by packing against the ligand and so holds the xylose moiety stably in place. The hydrogen bonding of the inhibitor is presented in more detail in Figures 4a and 5a.

X-O-C_4. The original electron density map suggested a binding to Glu177 although the electron density was not

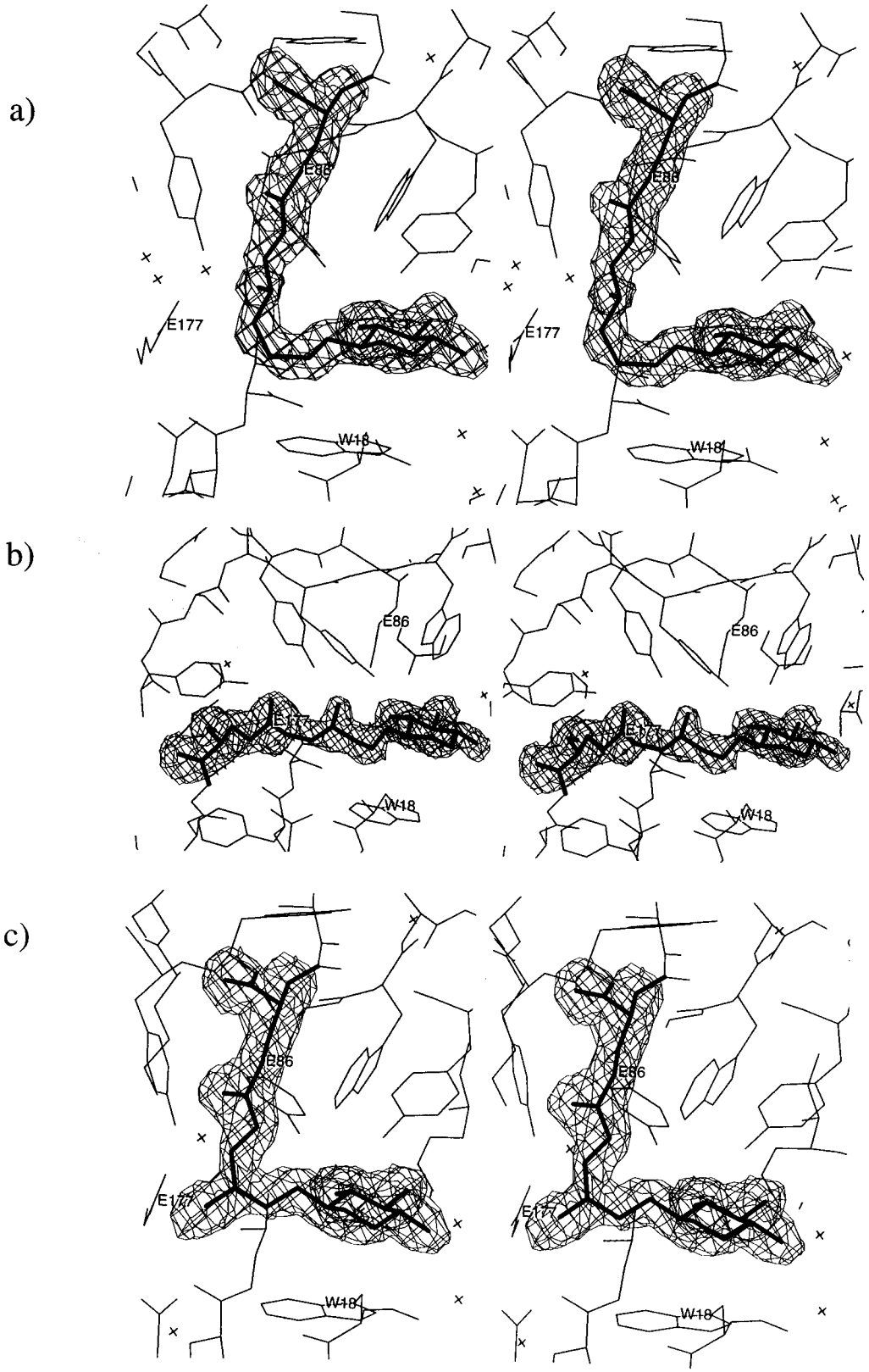

FIGURE 3: The omit electron density maps (coefficient $F_{obs} - F_{calc}$) around the ligand and the corresponding glutamic acid residue (drawn using XtalView; McRee, 1992). All the maps are contoured at 2.5σ level and superimposed on the final atomic model: (a) X-O-C_5; (b) X-O-C_4; (c) X-O-C_3.

continuous. The refinement process improved the ligand electron density confirming the binding of the ligand (Figure 3b). The binding of the xylose moiety is similar to that in the complex structure X-O-C_5. The hydroxyl group of the hydroxyl ester formed is hydrogen-bonded to the side chains of the residues Tyr88, Tyr77, and the catalytic residue Glu86 (Figures 4b and 5b). A somewhat obscure electron density was also observed on the other side of the active site, and it may indicate weak ligand binding also to the subsites +2 and +1.

X-O-C_3 binds convalently to the side chain of the catalytic residue Glu86 (Figure 3c). The xylose moiety is stabilized

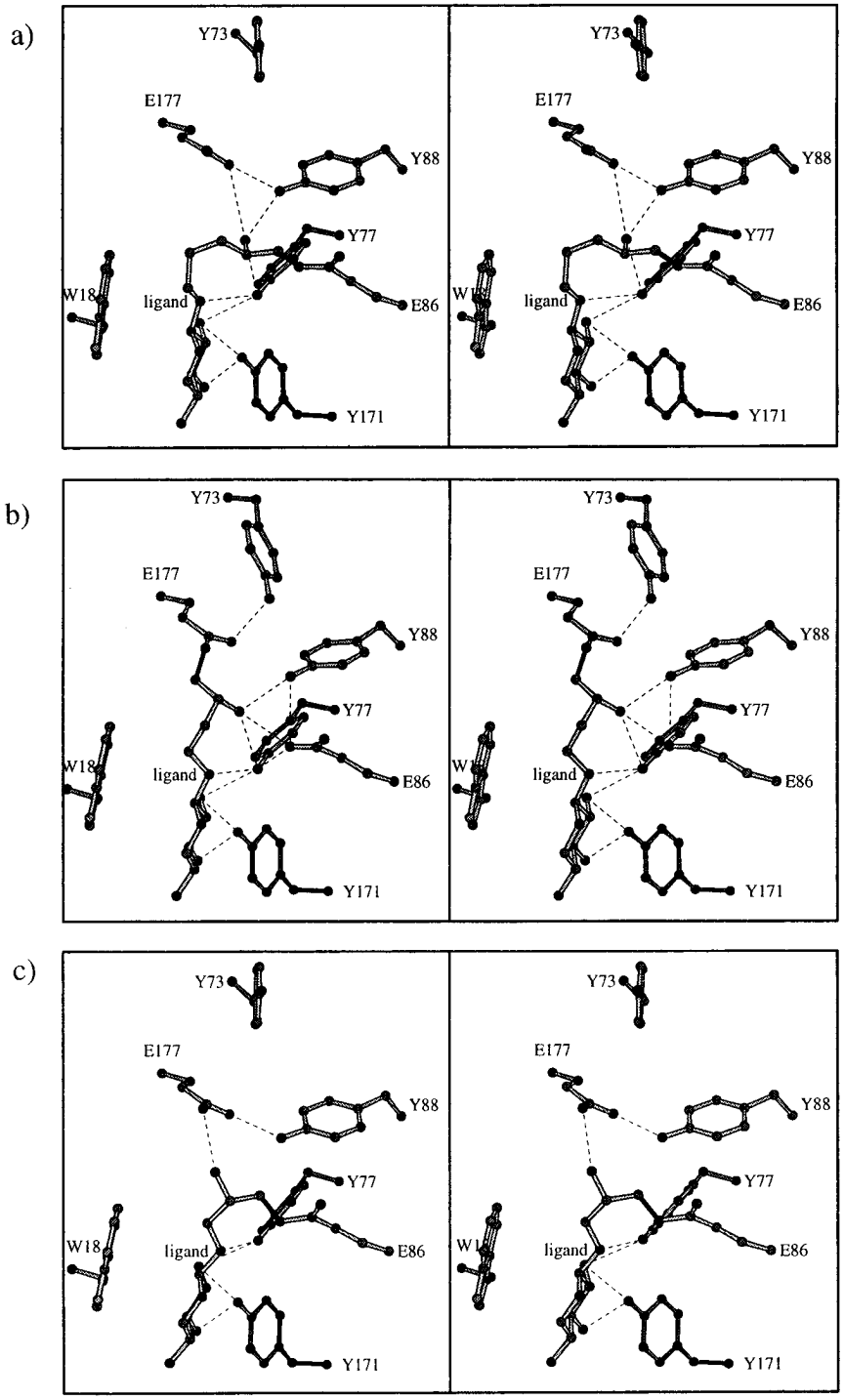

FIGURE 4: Binding of ligands in the active site of XYNII. (a) X-O-C_5, (b) X-O-C_4, and (c) X-O-C_3. Figures are drawn with Molscript (Kraulis, 1991).

by hydrogen bonds to the residues Tyr77 and Tyr171, and the ether oxygen forms a hydrogen bond with the residue Tyr77. The hydroxyl group formed is hydrogen-bonded to the catalytic residue Glu177. Moreover, the catalytic residue Glu177 and residue Tyr88 are also hydrogen-bonded. Trp18 packs against the xylose moiety as is the case in the two other complex structures, X-O-C_4 and X-O-C_5 (Figures 4c and 5c). The twisted aglycon stretched over subsite −1 and the torsion angles of the chain are all staggered or near staggered.

Binding of Benzoic Acid. In the first complex structure determined, X-O-C_5, a large flat electron density was observed between the two XYNII molecules, A and B, in the asymmetric unit. The discovered electron density was suspected to be benzoic acid, which appeared as an inpurity in the inhibitor solution. To confirm the coordination of benzoic acid, a crystal was soaked in benzoic acid solution, a data set collected, and the structure refined (Tables 1 and 2). The initial difference electron density map had previously showed similar flat electron density between the A and B molecules, as observed in the all three complex structures. The benzoic acid molecule binds in the small cavity between the A and B molecules and forms hydrophobic contacts with six residues, namely, with three N-terminal residues, Gln1, Thr2, and Ile3, of molecule B and with three residues, Lys104, Gly106, and Glu107, of the A molecule. The

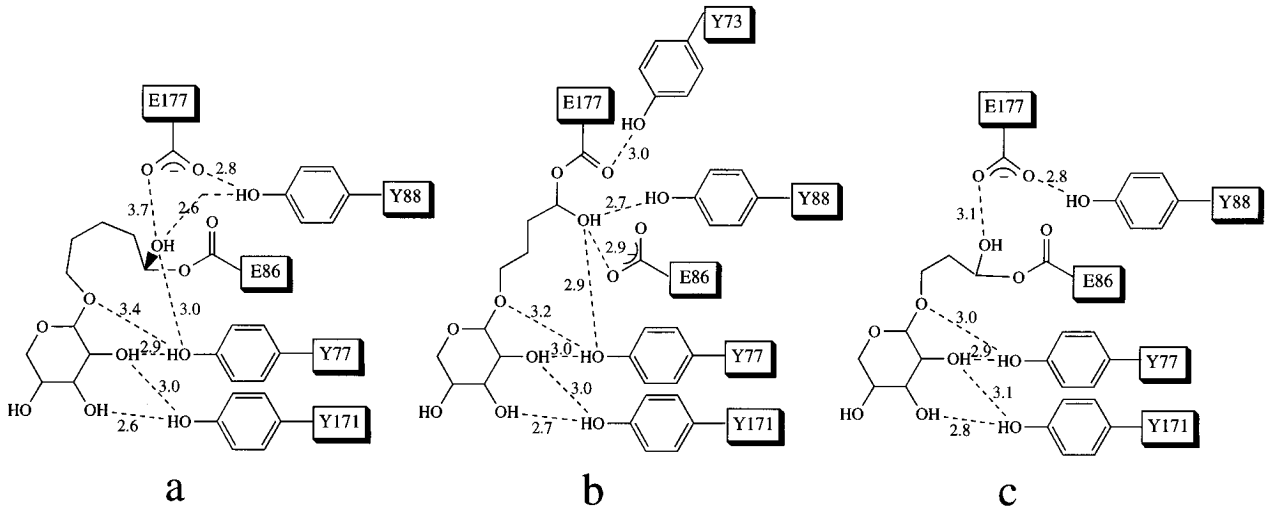

FIGURE 5: Hydrogen-bonding of the ligands in the active site cleft of XYNII: (a) X-O-C_5, (b) X-O-C_4, and (c) X-O-C_3. The distances between non-hydrogen atoms are given in angströms (Å).

Table 3: The rms Differences between Xylanase Molecules[a]

(a) Between A Xylanase Molecules

		native A			complex A		
	pH	pH 4.5	pH 6.0	pH 6.5	X-O-C_5	X-O-C_4	X-O-C_3
native A	4.5		0.092	0.158	0.221	0.190	0.318
native A	6.0			0.099	0.176	0.153	0.278
native A	6.5				0.128	0.116	0.237
X-O-C_5 A	6.1					0.092	0.162
X-O-C_4 A	5.3						0.181
X-O-C_3 A	5.8						

(b) Between B Xylanase Molecules

		native B			complex B		
	pH	pH 4.5	pH 6.0	pH 6.5	X-O-C_5	X-O-C_4	X-O-C_3
native B	4.5		0.081	0.128	0.321	0.274	0.580
native B	6.0			0.094	0.314	0.274	0.581
native B	6.5				0.273	0.240	0.534
X-O-C_5 B	6.1					0.138	0.342
X-O-C_4 B	5.3						0.350
X-O-C_3 B	5.8						

(c) Between A and B Xylanase Molecules

		native A			complex A		
	pH	pH 4.5	pH 6.0	pH 6.5	X-O-C_5	X-O-C_4	X-O-C_4
native B	4.5	0.244	0.249	0.276	0.272	0.249	0.276
native B	6.0	0.240	0.231	0.251	0.249	0.228	0.253
native B	6.5	0.272	0.246	0.242	0.226	0.215	0.212
X-O-C_5 B	6.1	0.484	0.451	0.430	0.386	0.340	0.314
X-O-C_4 B	5.3	0.422	0.394	0.378	0.389	0.340	0.285
X-O-C_3 B	5.8	0.690	0.653	0.612	0.562	0.574	0.491

[a] The three native structures measured at different pH have been determined earlier (Törrönen et al., 1995).

coordination of the benzoic acid did not influence the conformation of XYNII but was an interesting side observation.

Changes in the Enzyme Structure. The conformational changes were analyzed by calculating the rms difference from Cα atoms between all the refined individual A or B molecules (Table 3) by using the lsq option of the program O (Jones et al., 1991). The effect of ligand binding is clearly seen in these numbers. The striking feature was that all the ligands bound only to molecule B. In spite of this, small changes in molecule A were also observed (0.116−0.318 Å) compared to the nonliganded A molecule (Table 3a). Ligand binding to molecule B causes a change which is

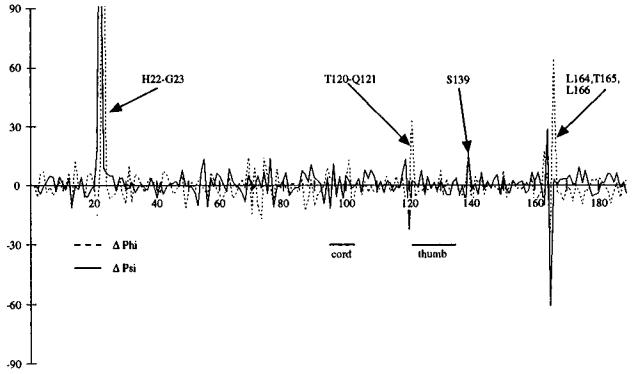

FIGURE 6: The differences of the ϕ and ψ main chain torsion angles between the native A molecule (measured at pH 4.5) and the B molecule complexed with X-O-C_3.

approximately 2 times larger (0.240−0.581 Å) (Table 3b). There are also differences between the three ligands used. The change was smallest in X-O-C_4 (0.240−0.274 Å) and slighly larger in X-O-C_5, whereas X-O-C_3 caused a significantly greater change in the whole structure (0.534−0.584 Å). The largest difference was found when comparing molecule A measured at pH 4.5 and molecule B complexed with X-O-C_3 (0.690 Å). The conformational changes were studied further by calculating the difference in the main chain dihedral torsion angles between the native molecule A (pH 4.5) and the molecule B complexed with X-O-C_3 (Figure 6). The peptide flip between His22 and Gly23 in the fingers region (Figure 2b) caused the largest change. This change has been observed constantly between A and B molecules, and it is probably not related to the movement of the thumb. There are no significant changes in the backbone torsion angles in the thumb region but slightly larger changes in the residues just before (Thr120 and Gln121) and after (Ser139) the thumb polypeptide region. In addition, the changes can be observed in the irregular polypeptide structure, namely, in Leu164, Thr165, and Leu166, following the α-helix.

When analyzing different conformations, we soon realized that these differences are related to the position of the "thumb", a long irregular structure which closes the active site (Figure 2a). As a measure of the movement or closeness of the "thumb", the distance between two atoms, Cγ of Pro126 and Cζ2 or Trp18, on the opposite side of the active site cleft were calculated (Table 4). The calculated distance

Table 4: The Closeness of the Thumb: The Distance (Å) between Cγ or Pro126 and Cζ2 of Trp18

PDB code	structure	molecule A	molecule B
1XYO	native pH 4.5	7.4	6.7
1ENX	native pH 6.0	7.2	6.7
1XYP	native pH 6.5	7.3	6.7
1RED	X-O-C_5	7.0	5.5
1REE	X-O-C_4	7.0	5.5
1REF	X-O-C_3	6.7	4.8

was largest in the native A molecule, 7.4 Å. The native B molecule is more closed, the distance being 6.7 Å. In complexed molecule B the distances for X-O-C_5, X-O-C_4, and X-O-C_3 were calculated to be 5.1, 5.5, and 4.6 Å, respectively. Thus the binding of the shortest ligand, X-O-C_3, caused the movement in the position of the "thumb". Especially the highly conserved side chain Tyr137 and Leu164 had undergone a conformational change. Tyr137 is located in the β-strand, next to the loop region forming the "thumb" of the imaginary "right hand". The residue Tyr137 turned at about 90° as a consequence of the movement of the whole loop region (Figure 2b).

DISCUSSION

Ligand Binding. In all the measured complex structures the inhibitor was bound only to molecule B in the asymmetric unit. By inspecting the packing of the molecules, it was concluded that this is probably not due to the crystal packing which could prevent the ligand molecule from binding to the active site of molecule A. The most likely explanation for the ligand binding only to molecule B is that the two molecules, A and B, in the asymmetric unit have slightly different conformations. The thumb has closed the active site a little bit more in molecule B than in molecule A. However, the difference is small as indicated by the distance between Cγ of Pro126 and Cζ2 of Trp18 which is approximately 0.5 Å shorter in molecule B than in molecule A. Yet, the final reason for the observed differences in the ligand binding in the XYNII crystals remains open.

The measurement of three complex structures showed interesting similarities but also differences in ligand binding. In all three cases the xylose residue binding to subsite −2 was very similar; for example, the hydrogen bonds with Tyr77 and Tyr171 as well as the packing with Trp18 were the same. It is thus clear that the xylose residue dictates the binding of the compounds and the binding of the different aglycon chains can vary. The aglycon occupies subsite −1, and although the lengths of the aliphatic side chain varies, the ligand can adopt a suitable conformation for binding to the active site. In the X-O-C_5 complex the aliphatic chain is strongly twisted reaching the nucleophilic Glu86. The X-O-C_4 complex represents an intermediate stage where it is probably incapable of adopting a suitable conformation to form a covalent bond with Glu86 but is in a favourable position toward an acid/base catalyst, Glu177. The shortest ligand, X-O-C_3, seems to fit best into the active site reaching Glu86. In this structure the thumb was the most closed.

More detailed information for the similar mechanism-based inhibitor is available only for 3,4-epoxybutyl β-D-cellobioside bound to the active site of *Bacillus* 1,3-1,4-glucanase (Keitel et al., 1993). In this case the ligand has formed a covalent link with the catalytic nucleophile. The binding of this ligand might be more unfavorable than the used XYNII ligands because many dihedral torsions are eclipsed.

So far, only one ligand−enzyme complex structure in family G xylanases has been published (Wakarchuk et al., 1994). In this study xylotetraose was soaked in the crystal of the inactive mutant (Glu172Cys) of *Bacillus circulans* xylanase. The study showed electron density in two subsites (corresponding to subsites −2 and −1). The xylose ring in subsite −2 binds in a similar manner to the xylose residue in XYNII complexes. The inhibitors aglycon-spanning subsite −1 in XYNII occupy an analogous position to the second xylose ring in the vicinity of the glutamic acid residues Glu78 and Glu172 to the *B. circulans* complex structure.

Conformational Changes. We previously determined three native XYNII structures at pH 4.5, 6.0, and 6.5 (Törrönen et al., 1995). In this study we have determined three XYNII complex structures. One alternative to compare structure is to use the rms difference (Table 3). When comparing different values, one must keep in the mind that the average coordinate error of the structures is approximately 0.2 Å. Some of the calculated differences are thus very small, but all together they may give a general view about the different conformations observed in XYNII crystals. In these six structures we can observe three kinds of conformational changes. These are due to (1) the crystal packing, (2) pH change, and (3) ligand binding. Some of the changes are local, for example, the specific side chain movements or movements in the position of the "thumb".

The influence of crystal packing is reflected in the differences between the A and B molecules (Table 3c). In the native structures the rms differences between the molecules are in the same range, 0.231−0.276 Å. The ligand binding to molecule B does not seem to affect the conformation of the unliganded A molecule because the rms difference between the A molecule from the complex structures and the B molecule from the native structures are in the same range, 0.212−0.276 Å.

The pH change in particular caused the conformational change in the catalytic residue Glu177 (Törrönen et al., 1994). The magnitude of this change can be estimated by comparing different native A and A or B and B molecules. In these structures, the rms difference is small, 0.092−0.158 Å, probably within the experimental error limits (Table 3a and 3b).

In this study we can now estimate the effect of ligand binding on the structure of XYNII. When we compare liganded B molecules and native B molecules, the rms difference is 0.273−0.534 Å. The change is thus significantly larger than the changes due to the pH change or crystal packing. By comparing the structures, it is quite obvious that these changes are especially due to the changes around the active site. The conformational change is also related to the ligand used. In X-O-C_4 the change was smallest compared to native molecules (0.240−0.274 Å) whereas in X-O-C_3 the change was largest (0.534−0.581 Å). The latter case probably better resembles the binding of the natural substrate, xylan. We could identify changes both in the main chain torsion angles (Figure 6) and in the side chain torsion angles, especially in Tyr137 and Leu164. These changes are concentrated mainly in the area on the base of the thumb (Figure 2b). It is possible that this region forms part of the hinge which regulates the closing or opening of the thumb.

The family 11/G xylanases (Henrissat et al., 1993; Törrönen et al., 1993a) all have highly conserved catalytic residues and a unique fold typical to them. As a result of this study, it can be suggested that the family 11/G xylanases function in a similar manner in the case of the enzyme changing the conformation when binding the substrate. The trigger for the conformational change is probably the substrate binding to the active site especially to the subsites −1 and −2. In particular in the case of XYNII the packing of Trp11 against the xylose ring seems to be important for the triggering.

Implications for Catalysis. Generally, the most retaining glycosidases employ a pair of carboxylic acid residues, aspartate or glutamate, as a catalytic residue. One of them functions as a general acid and a general base while the other acts as a nucleophile (McCarter & Withers, 1994). The importance of the two completely conserved glutamic acid residues (corresponding to Glu86 and Glu177 in XYNII) in the catalysis among family 11/G xylanases has been demonstrated earlier by site-directed mutagenesis studies (Wakarchuk et al., 1994). On the basis of hydrogen-bonding pattern, it was deduced that Glu86 is a possible nucleophile and Glu177 an acid/base catalyst (Törrönen et al., 1995).

Høj et al. have proposed a reaction mechanism for the covalent attachment of the epoxyalkyl inhibitor at the active site of *Bacillus subtilis* endohydrolase (Høj et al., 1989). In this scheme the epoxide oxygen corresponds to the glycosidic oxygen and the reaction starts when the acid catalyst donates a proton to this oxygen. This is followed by a nucleophilic attack from another active site residue, the nucleophilic carboxylate anion (aspartate or glutamate), leading to the formation of a covalent bond between the ligand and enzyme. This scheme applies to X-O-C_5 and X-O-C_3 complexes but not to X-O-C_4, where the covalent bond is formed between the acid/base catalyst Glu177 and the ligand. In fact, after donating a proton, Glu177 is also a carboxylate anion, a putative nucleophile competing with another nucleophile, Glu86. The results show that epoxide compounds can react with both the nucleophile and the acid/base catalyst. The alkyl chains of the used ligands are quite flexible. Therefore, they all are capable of adopting the range of different conformations. In all three cases one conformation exists where the epoxide ring is in the favorable position toward Glu86 or Glu177 but not both resulting in the covalent bond. One of the conformations of X-O-C_4 seems to be able to bind also to subsites +2 and +1 and make the covalent bond with Glu177. Therefore, although the xylose ring binds specifically to XYNII, the alkyl chain does not, and this makes the different binding modes possible.

The different covalent binding of the epoxide xylosides used indicates that the reaction mechanisms must be slightly different. Recently, Kuroki et al. have shown that the reaction mechanism of another glycosidase, T4 lysozyme, can be changed by site-directed mutagenesis (Kuroki et al., 1995). This study suggests that the reaction mechanism can also be affected by changing the ligand although XYNII works with a single mechanism with natural substrate. In addition, this study has indicated that the epoxide xylosides cannot be used to label the catalytic nucleophile.

ACKNOWLEDGMENT

We thank Ms. Reetta Kallio for her skillful technical assistance.

REFERENCES

Brünger, A. T., Kuriyan, J., & Karplus, M. (1987) *Science 235*, 458−460.
Chen, L., Garrett, T. P. J., Fincher, G. B., & Høj, P. B. (1995) *J. Biol. Chem. 270*, 8093−8101.
Clarke, A. (1988) *Biochem. Cell. Biol. 66*, 871−879.
Davies, G., & Henrissat, B. (1995) *Structure 3*, 853−859.
Henrissat, B.,& Bairoch, A. (1993) *Biochem. J. 293*, 781−788.
Høj, P. B., Rodriguez, E. B., Stick, R. V., & Stone, B. A. (1989) *J. Biol. Chem. 264*, 4939−4947.
Høj, P. B., Rodriguez, E. B., Iser, J. R., Stick, R. V., & Stone, B. A. (1991) *J. Biol. Chem. 266*, 11628−11631.
Høj, P. B., Condron, R., Traeger, J. C., McAuliffe, J. C., & Stone, B. A. (1992) *J. Biol. Chem. 266*, 25059−25066.
Jones, T. A., Zhou, J.-Y., Cowan, S. W., & Kjeldgaard, M. (1991) *Acta Crystallogr. A47*, 110−119.
Keitel, T., Simon, O., Borriss, R., & Heinemann, U. (1993) *Proc. Natl. Acad. Sci. U.S.A. 90*, 5287−5291.
Kraulis, P. J. (1991) *J. Appl. Crystallogr. 24*, 946−950.
Kuroki, R., Weaver, L. H., & Matthews, B. W. (1995) *Nature, Struct. Biol. 2*, 1007−1011.
McCarter, J. D., & Withers, S. G. (1994) *Curr. Opin. Struct. Biol. 4*, 885−892.
McRee, D. E. (1992) *J. Mol. Graph. 10*, 44−46.
Sato, M., Yamamoto, M., Imada, K., & Katsube, Y. (1992) *J. Appl. Crystallogr. 25*, 348−357.
Tenkanen, M., Puls, J., & Poutanen, K. (1992) *Enzyme Microb. Technol. 14*, 566−574.
Törrönen, A., & Rouvinen, J. (1995) *Biochemistry 34*, 847−856.
Törrönen, A., Kubicek, C. P., & Henrissat, B. (1993a) *FEBS Lett. 321*, 135−139.
Törrönen, A., Rouvinen, J., Ahlgren, M., Harkki, A., & Visuri, K. (1993b), *J. Mol. Biol. 233*, 313−316.
Törrönen, A., Harkki, A., & Rouvinen, J. (1994), *EMBO J. 13*, 2493−2501.
Wakarchuk, W. W., Campbell, R. L., Sung, W. L., Davodi, J., & Yaguchi, M. (1994) *Protein Sci. 3*, 467−475.
Wang, Q., Graham, R. W., Trimbur, D., Warren, R. A. J., & Withers, S. G. (1994) *J. Am. Chem. Soc. 116*, 11594−11595.

BI953052N